

# Precisely measuring the orbital angular momentum of beams via weak measurement

Jiangdong Qiu,<sup>1,2</sup> Changliang Ren,<sup>2,\*</sup> and Zhiyou Zhang<sup>1,†</sup>

<sup>1</sup>Key Laboratory of High Energy Density Physics and Technology of Ministry of Education, Sichuan University, Chengdu 610064, China

<sup>2</sup>Chongqing Institute of Green and Intelligent Technology, Chinese Academy of Sciences, People's Republic of China

(Received 7 March 2016; published 23 June 2016)

We proposed and analyzed a scheme of precisely measuring orbital angular momentum (OAM) of the vortex beams with the help of weak measurement process. The orbital angular momentum information  $l$  of the unknown OAM state can be obtained by its spatial displacements. The valid condition of precisely measuring orbital angular momentum was completely discussed. Interestingly, it is shown that the measurement by using the two-dimensional spatial displacements jointly is very useful for precisely measuring the OAM state with a large orbital angular momentum  $l$ . The signal-to-noise ratio of the measurement can be enhanced by increasing the weak-coupling  $\gamma$  linearly as the valid condition is still satisfied. For fixed  $\gamma$ , the maximal signal-to-noise ratio for each weak value increases with the decrease of the weak value.

DOI: [10.1103/PhysRevA.93.063841](https://doi.org/10.1103/PhysRevA.93.063841)

## I. INTRODUCTION

The orbital angular momentum (OAM) state, expressed by a phase cross section of  $\exp(il\phi)$  with  $l$  taking any integer value, carries an orbital angular momentum of  $l\hbar$ . Beams carrying orbital angular momentum, also called vortex beams, are attracting more and more attention in a wide field due to their unique characteristics, which have significant potential applications in optical manipulation [1], optical communication [2], quantum cryptography [3], quantum information [4], quantum memory [5], manipulating nanoparticles [6], determining chirality of crystals [7], and increase new possibilities to explore the interaction of electrons with magnetism [8–11].

In order to realize these applications experimentally, The most crucial question is how to produce high quality OAM beams and precisely measure them. Some of the previous investigations have been done on the generation of the OAM state for different particles such as photons [12–20], electrons [21–26], and atoms [27]. Various methods of measuring the OAM state have been proposed during the last twenty years, such as in optical systems [28] and in electronic systems [29–31]. Unfortunately, there are few works involved in analyzing precisely the measurement of the OAM state with a large orbital angular momentum  $l$ . As we know that the measurement of the OAM state will become more difficult with the increase of orbital angular momentum  $l$ , it is worthwhile to extend some different methods to solve this problem.

As a different experimental technique, weak measurement [32] may be one alternative way of tackling this problem. Various previous investigations have been shown that weak measurement is an especially useful measuring method, which has been used to measure wave function [33], realize signal amplification [34], and resolve the Hardy paradox [35]. Recently, weak measurement has used the OAM state as the pointer, which can help extract weak values of higher-order moments of single-particle operators [36], joint weak values [37], and information on the polarization state from the single image [38]. Conversely thinking, it is reasonable

to consider a method of precisely measuring the OAM state with the help of weak measurement process. Inspired by such a consideration, we propose coupling the OAM state with a well-defined pre- and postselected system, which creates an indirect coupling between  $X$ ,  $Y$ , and OAM  $l$ . Hence, we can get OAM  $l$  by using the spatial displacements. A complete analysis and discussion is done. It is shown that this method is very useful for precisely measuring the OAM state with a large orbital angular momentum  $l$ . In Sec. II, we explain the basic theoretical description of OAM measurement protocol, and in Sec. III we show how to extract the orbital angular momentum information and analyze this method in detail.

## II. BASIC THEORETICAL DESCRIPTION OF OAM MEASUREMENT PROTOCOL

Without loss of generality, suppose that the unknown OAM state is expressed as

$$\psi_m(x, y) = \frac{\sqrt{2^{l+1}}}{\sigma \sqrt{\pi l!}} \left( \frac{x + iy}{\sigma} \right)^l \exp\left(-\frac{x^2 + y^2}{\sigma^2}\right), \quad (1)$$

where  $\frac{\sqrt{2^{l+1}}}{\sigma \sqrt{\pi l!}}$  is the normalized coefficient,  $l$  is the topological charge, and  $l \geq 0$  is assumed for simplicity. So definitely our main goal is getting the precise information of  $l$ . As we plan to carry out such measurement with the help of weak measurement, the theoretical measurement procedure is similar to a weak measurement protocol with an OAM pointer. The only difference is that the weak value is well defined using the well-controlled pre- and postselection process. Then consider the weak interaction between the observable  $\hat{A}$  system initially prepared in the state  $\rho = |\psi\rangle\langle\psi|$  with the unknown OAM state Eq. (1). Hence, the total initial state is  $\rho_{in} = \rho \otimes \rho_m$ , where  $\rho_m = |\psi_m\rangle\langle\psi_m|$ . In the von Neumann measurement scheme, the interaction between them is described by the Hamiltonian

$$H = \gamma \hat{A} \otimes \hat{P}_x, \quad (2)$$

where  $\gamma$  is the coupling constant, and  $\hat{P}_x$  is the momentum observable of the unknown OAM state conjugate to position observable  $\hat{X}$ . Assuming that  $\hat{A}^2 = \hat{I}$ , which has been discussed in detail [39] and realized in many experiments [34,38],

\*Corresponding author: renchangliang@cigit.ac.cn

†Corresponding author: zhangzhiyou@scu.edu.cn

the unitary operator can be described as

$$U = \cos(\gamma \hat{P}_x) - i \hat{A} \sin(\gamma \hat{P}_x). \quad (3)$$

The total initial state undergoes unitary transformation and becomes  $\rho_f = |\psi_f\rangle\langle\psi_f| = U\rho \otimes \rho_m U^\dagger$ . After postselection  $\Pi_\phi = |\phi\rangle\langle\phi|$  on the  $\hat{A}$  system, we can get the probability distribution of the final state,

$$\Phi_p(x, y) = \frac{\langle \Pi_\phi \otimes \Pi_{x,y} \rangle_f}{\langle \Pi_\phi \rangle_f}, \quad (4)$$

where  $\Pi_{x,y} = |x, y\rangle\langle x, y|$  is the projection operator in position space,  $\langle \Pi_\phi \otimes \Pi_{x,y} \rangle_f = \text{Tr}[(\Pi_\phi \otimes \Pi_{x,y})\rho_f]$ , and  $\langle \Pi_\phi \rangle_f = \text{Tr}[\Pi_\phi \rho_f]$  is the normalization coefficient. Taking Eq. (3) into Eq. (4), we can obtain the numerator

$$\begin{aligned} \langle \Pi_\phi \otimes \Pi_{x,y} \rangle_f &= |\langle \phi | \psi \rangle|^2 \{ |\psi_{mc}|^2 + 2\text{Im}(A_w \psi_{mc}^* \psi_{ms}) \\ &\quad + |A_w|^2 |\psi_{ms}|^2 \}, \end{aligned} \quad (5)$$

where  $\psi_{mc} = \langle x, y | \cos(\gamma P_x) | \psi_m \rangle$ ,  $\psi_{ms} = \langle x, y | \sin(\gamma P_x) | \psi_m \rangle$ , and the normalization

$$\begin{aligned} \langle \Pi_\phi \rangle_f &= |\langle \phi | \psi \rangle|^2 \left\{ \frac{1}{2} + \frac{1}{2} |A_w|^2 + \overline{\sin(2\gamma \hat{P}_x)} \text{Im} A_w \right. \\ &\quad \left. + \frac{1}{2} \overline{\cos(2\gamma \hat{P}_x)} (1 - |A_w|^2) \right\}, \end{aligned} \quad (6)$$

where the  $\overline{\cos(2\gamma \hat{P}_x)}$ , and the  $\overline{\sin(2\gamma \hat{P}_x)}$  are represented by  $\langle \psi_m | \cos(2\gamma \hat{P}_x) | \psi_m \rangle$ ,  $\langle \psi_m | \sin(2\gamma \hat{P}_x) | \psi_m \rangle$  respectively.

Considering the relationship  $\cos(\gamma \hat{P}_x) = \frac{e^{-i\gamma \hat{P}_x} + e^{i\gamma \hat{P}_x}}{2}$ ,  $\sin(\gamma \hat{P}_x) = i \frac{e^{-i\gamma \hat{P}_x} - e^{i\gamma \hat{P}_x}}{2}$ , and  $\psi_m(x - \gamma, y) = \langle x, y | e^{-i\gamma \hat{P}_x} | \psi_m(x, y) \rangle$ , the numerator Eq. (5) becomes

$$\begin{aligned} \langle \Pi_\phi \otimes \Pi_{x,y} \rangle_f &= |\langle \phi | \psi \rangle|^2 \left\{ \frac{1}{4} (1 - 2\text{Re}A_w + |A_w|^2) \phi(x + \gamma, y) \right. \\ &\quad + \frac{1}{4} (1 + 2\text{Re}A_w + |A_w|^2) \phi(x - \gamma, y) \\ &\quad + \frac{1}{2} (1 - |A_w|^2) \text{Re}([\psi_m^*(x + \gamma, y) \psi_m(x - \gamma, y)]) \\ &\quad \left. + \text{Im}A_w \text{Im}([\psi_m^*(x + \gamma, y) \psi_m(x - \gamma, y)]) \right\}, \end{aligned} \quad (7)$$

where  $\phi(x, y)$  is the meter initial probability distribution denoted by  $|\psi_m(x, y)|^2$ .  $A_w$  is the weak value [32,40] defined as

$$A_w = \frac{\langle \phi | \hat{A} | \psi \rangle}{\langle \phi | \psi \rangle}. \quad (8)$$

Based on Eqs. (6) and (7), we can derive the average spatial displacements after the postselection process. Without any approximation, the explicit average spatial displacements, calculated by the integral  $\int x \Phi_p(x, y) dx dy$  and  $\int y \Phi_p(x, y) dx dy$ , can be written as

$$\bar{x} = \frac{2\gamma \text{Re}A_w}{1 + |A_w|^2 + \mathbf{b} \exp(-2\frac{\gamma^2}{\sigma^2})(1 - |A_w|^2)}, \quad (9)$$

$$\bar{y} = \frac{-2\gamma \mathbf{a} \text{Im}A_w \exp(-2\frac{\gamma^2}{\sigma^2})}{1 + |A_w|^2 + \mathbf{b} \exp(-2\frac{\gamma^2}{\sigma^2})(1 - |A_w|^2)}, \quad (10)$$

are the polynomials expressed as

$$\begin{aligned} \mathbf{a} &= \sum_{n=0}^{\frac{l-1}{2}} \sum_{m=0}^{l-2n-1} \sum_{k=0}^m \frac{(-1)^{l-m-n} 2^{l-n-3m-2}}{(2n+1)!(l-2n-m-1)!(m-k)!k!} \\ &\quad \times \frac{[2(m-k)]![2(n+1+k)]!}{(m-k)!(n+k+1)!} \left( \frac{\gamma^2}{\sigma^2} \right)^{l-m-n-1}, \end{aligned} \quad (11)$$

$$\begin{aligned} \mathbf{b} &= \sum_{n=0}^{\lfloor l/2 \rfloor} \sum_{m=0}^{l-2n} \sum_{k=0}^m \frac{(-1)^{l-m-n} 2^{l-n-3m}}{(2n)!(l-2n-m)!(m-k)!k!} \\ &\quad \times \frac{[2(m-k)]![2(n+k)]!}{(m-k)!(n+k)!} \left( \frac{\gamma^2}{\sigma^2} \right)^{l-m-n}. \end{aligned} \quad (12)$$

We must point out that polynomial  $\mathbf{a}$  of Eq. (11) is valid for  $l > 0$ . For  $l = 0$ , the meter initial state is the fundamental Gaussian mode, hence there is no displacement in the  $y$  direction after postselection with  $\bar{y} = 0$ . Obviously, the explicit average spatial displacements Eqs. (9) and (10) carry the information of the orbital angular momentum  $l$  of the OAM state. However, the relationship between the explicit average spatial displacements and the orbital angular momentum is not distinct. We should show when and how we can extract the precise information of the OAM state. And the method of obtaining the orbital angular momentum from  $\bar{x}$  or  $\bar{y}$  independently is so trivial that many researchers knew it before. In the following section, we will explain and demonstrate a more efficient way to obtain more precise orbital angular momentum information.

### III. EXTRACTING AND ANALYZING THE ORBITAL ANGULAR MOMENTUM INFORMATION

Dividing Eq. (10) by Eq. (9), we can obtain that

$$\mathbf{a} = -\frac{\text{Re}A_w \bar{y}}{\text{Im}A_w \bar{x}} \exp\left(-2\frac{\gamma^2}{\sigma^2}\right). \quad (13)$$

This formula is the key that getting the information about the OAM  $l$ . The polynomial  $\mathbf{a}$  (11) is related to  $l$ . But it is not enough to determine the OAM with Eq. (13) alone. However, considering the weak-coupling condition  $\gamma \ll 1$ , we expand Eq. (11) to the first order in the parameter  $\frac{\gamma^2}{\sigma^2}$  with the higher terms neglected and we obtain

$$\mathbf{a} = l - l(l-1)\frac{\gamma^2}{\sigma^2}. \quad (14)$$

Jointly considering Eqs. (13) and (14), when the situation

$$l^2 \frac{\gamma^2}{\sigma^2} \ll 1 \quad (15)$$

is satisfied, the orbital angular momentum  $l$  only depends on the weak value  $A_w$  and average spatial displacements of the OAM state. Under the valid condition Eq. (15),  $\exp(-2\frac{\gamma^2}{\sigma^2}) \rightarrow 1$  and  $l(l-1)\frac{\gamma^2}{\sigma^2} \rightarrow 0$ , by using Eqs. (13) and (14), we get the accurate OAM  $l$ ,

$$l = -\frac{\text{Re}A_w \bar{y}}{\text{Im}A_w \bar{x}}. \quad (16)$$

Hence, it is clear that we can obtain the accurate OAM  $l$  from the measurements  $\bar{x}$  and  $\bar{y}$  with fixed weak value of  $\hat{A}$ .

It is reasonable to analyze the efficiency of this method. Definitely, we should compare its performance by obtaining orbital angular momentum  $l$  from  $\bar{x}$  or  $\bar{y}$  directly, as the back way is apparently more well reasoned. Similarly expanding the polynomial  $b$  Eq. (12) to the first order in parameter  $\frac{\gamma^2}{\sigma^2}$ , we can obtain that

$$b = 1 - 2l \frac{\gamma^2}{\sigma^2}. \quad (17)$$

By using Eq. (17) and the condition Eq. (15), the formulas about  $\bar{x}$  and  $\bar{y}$  can be rewritten as

$$\bar{x} \cong \frac{\gamma \operatorname{Re} A_w}{1 + l \frac{\gamma^2}{\sigma^2} |A_w|^2}, \quad (18)$$

$$\bar{y} \cong -\frac{\gamma \operatorname{Im} A_w l}{1 + l \frac{\gamma^2}{\sigma^2} |A_w|^2}. \quad (19)$$

Hence, we can get a simpler relation between the orbital angular momentum  $l$  and  $\bar{y}$ ,

$$\bar{y} = -\gamma \operatorname{Im} A_w l, \quad (20)$$

when the valid condition

$$l^2 \frac{\gamma^2}{\sigma^2} |A_w|^2 \ll 1 \quad (21)$$

is satisfied. Therefore, we can obtain the value  $l$  by measuring  $\bar{y}$  with fixed weak value. However, comparing the two valid conditions  $l^2 \frac{\gamma^2}{\sigma^2} \ll 1$  and  $l^2 \frac{\gamma^2}{\sigma^2} |A_w|^2 \ll 1$ , the first one is looser than the second one, so the measurement of orbital angular momentum  $l$  by using  $\bar{x}$  and  $\bar{y}$  jointly has a less strict condition than that of using  $\bar{y}$  alone. It will be very useful for precisely measuring the OAM state with a large orbital angular momentum  $l$ .

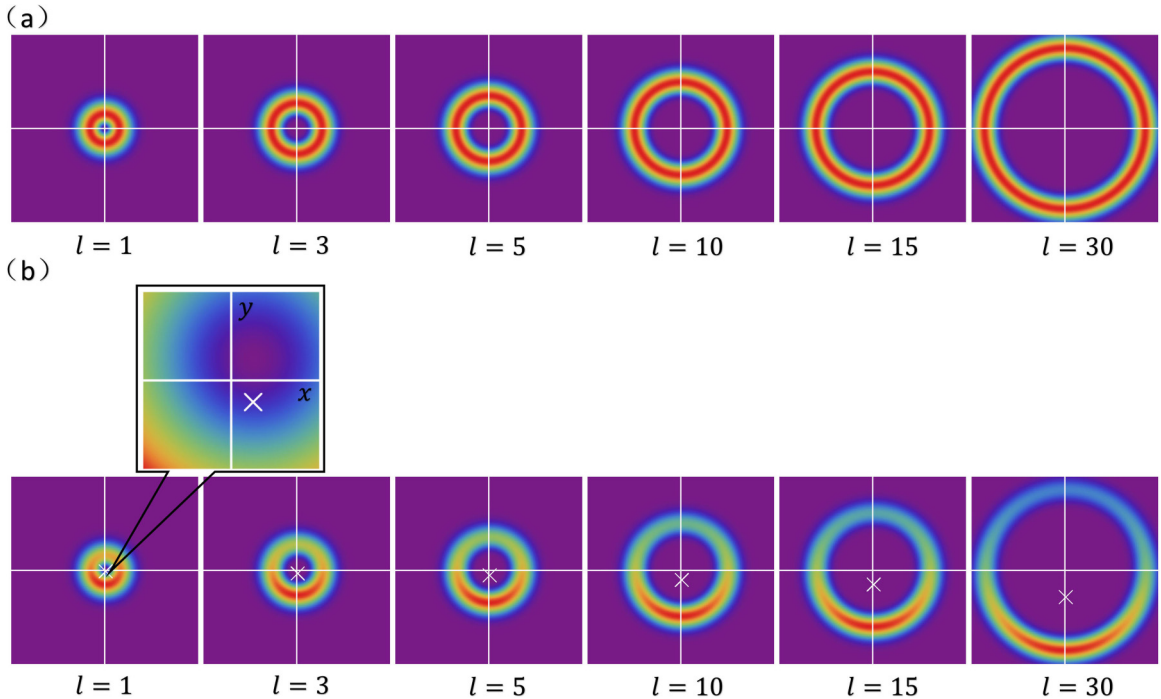


FIG. 1. Intensity distribution of the final state for different OAM states. (a) The intensity distribution with  $\gamma = 0$ , which is the same as the initial OAM state. (b) The intensity distribution of final state Eq. (28) with the parameters  $\eta = \theta = 0.2$ ,  $\sigma = 1$ ,  $\gamma = 0.01$ , where the white cross represents average position  $\bar{x}$ ,  $\bar{y}$ . The exact values  $\bar{x}$ ,  $\bar{y}$  are shown in Table I.

TABLE I. The value  $\bar{x}$ ,  $\bar{y}$  of the final state Eq. (28) with the parameters  $\eta = \theta = 0.2$ ,  $\gamma = 0.01$ ,  $\sigma = 1$  for different OAM and the measurement of orbital angular momentum using different methods.

OAM	1	3	5	10	15	30
$\bar{x}$	0.0498	0.0494	0.0489	0.0478	0.0467	0.0437
$\bar{y}$	-0.0488	-0.1451	-0.2395	-0.4677	-0.6854	-1.2822
$-\frac{\text{Re}A_w}{\text{Im}A_w} \frac{\bar{y}}{\bar{x}}$	0.9998	2.9988	4.997	9.9890	14.9760	29.9071
$\frac{-\bar{y}}{\gamma \text{Im}A_w}$	0.9902	2.9416	4.8553	9.4818	13.8949	25.9917

ratio can be increased by improving the interaction strength  $\gamma$  as the valid condition  $l^2 \frac{\gamma^2}{\sigma^2} \ll 1$  is still satisfied. When  $l^2 \frac{\gamma^2}{\sigma^2} |A_w|^2 \geq 1$ , the signal-to-noise ratio cannot be expressed as Eqs. (25) and (26); according to Eq. (24), the dominant factor of the signal-to-noise ratio is the weak value  $|A_w|$  and the effect of interaction strength  $\gamma$  is negligible.

Furthermore, we can devise a concrete example to present such characterization of this new OAM state measurement protocol directly. Assuming the system initial state  $|\psi\rangle = \exp(-i\frac{\theta}{2})|0\rangle + \exp(i\frac{\theta}{2})|1\rangle$  with the project operator  $\hat{A} = |0\rangle\langle 0| - |1\rangle\langle 1|$ , the system state interacts with one unknown OAM state as defined in Eq. (1). When we carry out a postselection measurement on the state  $|\phi\rangle = \cos(\eta/2 - \pi/4)|0\rangle + \sin(\eta/2 - \pi/4)|1\rangle$ , the weak value can be obtained as

$$A_w \cong 2 \frac{\eta}{\eta^2 + \theta^2} + 2 \frac{i\theta}{\eta^2 + \theta^2}, \quad (27)$$

when  $\theta, \eta \ll 1$ . After postselection measurement on the system, the final state can be expressed as

$$\begin{aligned} \psi_f(x, y) &= \langle \phi | e^{-i\gamma \hat{A} \otimes \hat{P}_x} |\psi\rangle |\psi_m\rangle \\ &= \exp\left(-i\frac{\theta}{2}\right) \cos(\eta/2 - \pi/4) \psi_m(x - \gamma, y) \\ &\quad + \exp\left(i\frac{\theta}{2}\right) \sin(\eta/2 - \pi/4) \psi_m(x + \gamma, y). \end{aligned} \quad (28)$$

We take the parameters  $\eta = \theta = 0.2$ ,  $\gamma = 0.01$ ,  $\sigma = 1$  of the final state, Eq. (28), shown in Fig. 1(b) for different OAM states. And the intensity distribution of the final state with  $\gamma = 0$ , which is the same as the initial OAM state, is shown in Fig. 1(a) for comparison.

Through numerical calculation, we obtain the value of two different formulas  $-\frac{\text{Re}A_w}{\text{Im}A_w} \frac{\bar{y}}{\bar{x}}$  and  $-\frac{\bar{y}}{\gamma \text{Im}A_w}$  for different  $l$  as shown in Table I. It shows that when the  $l$  is small, the two methods can both obtain the precise results. However, as  $l$  is large, the condition  $l^2 \frac{\gamma^2}{\sigma^2} \ll 1$  is still but the condition  $l^2 \frac{\gamma^2}{\sigma^2} |A_w|^2 \ll 1$  is not satisfied. Hence we can still obtain the precise orbital angular momentum information using the first method, while the second method will be invalid.

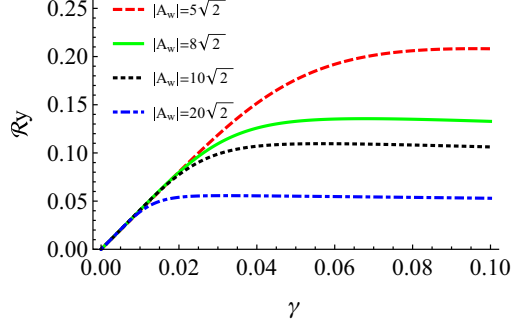


FIG. 2. The  $\Re y$  vs  $\gamma$  for different weak values  $A_w$ . Parameters  $\sigma = 1$ ,  $l = 5$ ,  $N = 1$ ,  $\eta = \theta = 0.05, 0.1, 0.125, 0.2$  corresponding to different weak values from blue to red line.

We also discuss the property of signal-to-noise ratio. Figure 2 shows the SNR Eq. (22) of  $y$  for different weak values  $A_w$  versus  $\gamma$ , where we choose the parameters  $\sigma = 1$ ,  $l = 5$ ,  $N = 1$ ,  $\eta = \theta = 0.05, 0.1, 0.125, 0.2$  corresponding to different weak values. It is shown that, when  $\gamma$  is small, the  $\text{SNR} \propto \gamma$  and the weak values have no influence on it which is coincident with (26). For fixed  $\gamma$ , the maximal signal-to-noise for each weak value increases with the decrease of the weak value.

#### IV. CONCLUSION

A scheme of precisely measuring the orbital angular momentum of the OAM state with the help of weak measurement process was proposed. The orbital angular momentum information  $l$  can be easily obtained by measuring the spatial displacements of the unknown OAM state with fixed weak value. The measurement of orbital angular momentum  $l$  by using  $\bar{x}$  and  $\bar{y}$  jointly has a less strict condition than that of using  $\bar{y}$  alone. Hence, the jointly spatial displacements measurement method can be used for precisely measuring the OAM state with a large orbital angular momentum  $l$ . The signal-to-noise ratio (SNR) of the measurement are discussed. When the valid condition is satisfied, the signal-to-noise ratio is linear to  $\gamma$  with fixed weak value. Therefore, the signal-to-noise ratio is enhanced by increasing the weak-coupling  $\gamma$  linearly as the valid condition is still satisfied. For fixed  $\gamma$ , we also found that the maximal signal-to-noise ratio for each weak value increases with the decrease of the weak value. This discussion not only provides one method of measuring OAM states, but also extends the application of weak measurement.

#### ACKNOWLEDGMENTS

C.L.R. acknowledges support by Youth Innovation Promotion Association of Chinese Academy of Sciences (China) Grant No. 2015317, Natural Science Foundations of Chongqing (China) (Grants No. cstc2013jcyjC00001, No. cstc2015jcyjA00021), and The project sponsored by SRF for ROCS-SEM (China) (Grant No. Y51Z030W10). Z.Z. acknowledges support by the National Natural Science Foundation of China (China) (Grant No. 11305111).

- [1] M. Padgett and R. Bowman, *Nat. Photon.* **5**, 343 (2011).
- [2] J. Wang, J.-Y. Yang, I. M. Fazal, N. Ahmed, Y. Yan, H. Huang, Y. Ren, Y. Yue, S. Dolinar, M. Tur, and A. E. Willner, *Nat. Photon.* **6**, 488 (2012).
- [3] S. Groblacher, T. Jennewein, A. Vaziri, G. Weihs, and A. Zeilinger, *New J. Phys.* **8**, 75 (2006).
- [4] A. Mair, A. Vaziri, G. Weihs, and A. Zeilinger, *Nature (London)* **412**, 313 (2001).
- [5] A. Nicolas, L. Veissier, L. Giner, E. Giacobino, D. Maxein, and J. Laurat, *Nat. Photon.* **8**, 234 (2014).
- [6] J. Verbeeck, H. Tian, and G. Van Tendeloo, *Adv. Mater.* **25**, 1114 (2013).
- [7] R. Juchtmans, A. Béché, A. Abakumov, M. Batuk, and J. Verbeeck, *Phys. Rev. B* **91**, 094112 (2015).
- [8] S. Lloyd, M. Babiker, and J. Yuan, *Phys. Rev. Lett.* **108**, 074802 (2012).
- [9] J. Rusz and S. Bhowmick, *Phys. Rev. Lett.* **111**, 105504 (2013).
- [10] K. Y. Bliokh, P. Schattschneider, J. Verbeeck, and F. Nori, *Phys. Rev. X* **2**, 041011 (2012).
- [11] M. Babiker, J. Yuan, and V. E. Lembessis, *Phys. Rev. A* **91**, 013806 (2015).
- [12] L. Allen, M. W. Beijersbergen, R. J. C. Spreeuw, and J. P. Woerdman, *Phys. Rev. A* **45**, 8185 (1992).
- [13] H. He, M. E. J. Friese, N. R. Heckenberg, and H. Rubinsztein-Dunlop, *Phys. Rev. Lett.* **75**, 826 (1995).
- [14] N. R. Heckenberg, R. McDuff, C. P. Smith, and A. G. White, *Opt. Lett.* **17**, 221 (1992).
- [15] M. W. Beijersbergen, R. Coerwinkel, M. Kristensen, and J. P. Woerdman, *Opt. Commun.* **112**, 321 (1994).
- [16] M. W. Beijersbergen, L. Allen, H. van der Veen, and J. P. Woerdman, *Opt. Commun.* **96**, 123 (1993).
- [17] N. González, G. Molina-Terriza, and J. P. Torres, *Opt. Express* **14**, 9093 (2006).
- [18] L. Marrucci, C. Manzo, and D. Paparo, *Phys. Rev. Lett.* **96**, 163905 (2006).
- [19] N. Yu, P. Genevet, M. A. Kats, F. Aieta, J. Tetienne, F. Capasso, and Z. Gaburro, *Science* **334**, 333 (2011).
- [20] W. Shu, D. Song, Z. Tang, H. Luo, Y. Ke, X. Lü, S. Wen, and D. Fan, *Phys. Rev. A* **85**, 063840 (2012).
- [21] K. Y. Bliokh, Y. P. Bliokh, S. Savelev, and F. Nori, *Phys. Rev. Lett.* **99**, 190404 (2007).
- [22] M. Uchida and A. Tonomura, *Nature (London)* **464**, 737 (2010).
- [23] J. Verbeeck, H. Tian, and P. Schattschneider, *Nature (London)* **467**, 301 (2010).
- [24] B. J. McMorran, A. Agrawal, I. M. Anderson, A. A. Herzing, H. J. Lezec, J. J. McClelland, and J. Unguris, *Science* **331**, 192 (2011).
- [25] L. Clark, A. Béché, G. Guzzinati, A. Lubk, M. Mazilu, R. Van Boxem, and J. Verbeeck, *Phys. Rev. Lett.* **111**, 064801 (2013).
- [26] V. Grillo, G. C. Gazzadi, E. Mafakheri, S. Frabboni, E. Karimi, and R. W. Boyd, *Phys. Rev. Lett.* **114**, 034801 (2015).
- [27] V. E. Lembessis, D. Ellinas, M. Babiker, and O. Al-Dossary, *Phys. Rev. A* **89**, 053616 (2014).
- [28] J. Leach, M. J. Padgett, S. M. Barnett, S. Franke-Arnold, and J. Courtial, *Phys. Rev. Lett.* **88**, 257901 (2002); G. C. G. Berkhout, M. P. J. Lavery, J. Courtial, M. W. Beijersbergen, and M. J. Padgett, *ibid.* **105**, 153601 (2010); P. Genevet, J. Lin, M. A. Kats and F. Capasso, *Nat. Commun.* **3**, 1278 (2012); A. Belmonte and J. P. Torres, *Opt. Lett.* **37**, 2940 (2012); K. Dai, C. Gao, L. Zhong, Q. Na, and Q. Wang, *ibid.* **40**, 562 (2015).
- [29] K. Saitoh, Y. Hasegawa, K. Hirakawa, N. Tanaka, and M. Uchida, *Phys. Rev. Lett.* **111**, 074801 (2013).
- [30] G. Guzzinati, L. Clark, A. Béché, and J. Verbeeck, *Phys. Rev. A* **89**, 025803 (2014).
- [31] L. Clark, A. Béché, G. Guzzinati, and J. Verbeeck, *Phys. Rev. A* **89**, 053818 (2014).
- [32] Y. Aharonov, D. Z. Albert, and L. Vaidman, *Phys. Rev. Lett.* **60**, 1351 (1988).
- [33] J. S. Lundeen, B. Sutherland, A. Patel, C. Stewart, and C. Bamber, *Nature (London)* **474**, 188 (2011).
- [34] O. Hosten and P. Kwiat, *Science* **319**, 787 (2008).
- [35] Y. Aharonov, A. Botero, S. Pospescu, B. Reznik, and J. Tollaksen, *Phys. Lett. A* **301**, 130 (2002); J. S. Lundeen and A. M. Steinberg, *Phys. Rev. Lett.* **102**, 020404 (2009); K. Yokota, T. Yamamoto, M. Koashi, and N. Imoto, *New J. Phys.* **11**, 033011 (2009).
- [36] G. Puentes, N. Hermosa, and J. P. Torres, *Phys. Rev. Lett.* **109**, 040401 (2012).
- [37] H. Kobayashi, G. Puentes, and Y. Shikano, *Phys. Rev. A* **86**, 053805 (2012).
- [38] H. Kobayashi, K. Nonaka, and Y. Shikano, *Phys. Rev. A* **89**, 053816 (2014).
- [39] K. Nakamura, A. Nishizawa, and M.-K. Fujimoto, *Phys. Rev. A* **85**, 012113 (2012).
- [40] A. G. Kofman, S. Ashhab, and F. Nori, *Phys. Rep.* **520**, 43 (2012).